analytical chemistry

Article

Cite This: Anal. Chem. 2018, 90, 12131−12136

pubs.acs.org/ac

Highly Sensitive Membraneless Fructose Biosensor Based on Fructose Dehydrogenase Immobilized onto Aryl Thiol Modified Highly Porous Gold Electrode: Characterization and Application in Food Samples

Paolo Bollella,*[,†] Yuya Hibino,[§] Kenji Kano,[§] Lo Gorton,[‡] and Riccarda Antiochia[†]

[†]Department of Chemistry and Drug Technologies, Sapienza University of Rome Piazzale Aldo Moro 5, 00185, Rome, Italy

[‡]Department of Analytical Chemistry/Biochemistry, Lund University, P.O. Box 124, 221 00, Lund, Sweden

[§]Division of Applied Life Sciences, Graduate School of Agriculture, Kyoto University, Sakyo, Kyoto 606-8502, Japan

Supporting Information

ABSTRACT: In this paper we present a new method to electrodeposit highly porous gold (h-PG) onto a polycrystalline solid gold electrode without any template. The electrodeposition is carried out by first cycling the electrode potential between +0.8 and 0 V in 10 mM $HAuCl_4$ with 2.5 M NH_4Cl and then applying a negative potential for the production of hydrogen bubbles at the electrode surface. After that the modified electrode was characterized in sulfuric acid to estimate the real surface area (A_{real}) to be close to 24 cm^2, which is roughly 300 times higher compared to the bare gold electrodes (0.08 cm^2). The electrode was further incubated overnight with three different thiols (4-mercaptobenzoic acid (4-MBA), 4-mercaptophenol (4-MPh), and 4-aminothiophenol (4-APh)) in order to produce differently charged self-assembled monolayers (SAMs) on the electrode surface. Finally a fructose dehydrogenase (FDH) solution was drop-cast onto the electrodes. All the modified electrodes were investigated by cyclic voltammetry both under nonturnover and turnover conditions. The FDH/4-MPh/h-PG exhibited two couples of redox peaks for the heme c_1 and heme c_2 of the cytochrome domain of FDH and as well as a well pronounced catalytic current density (about 1000 $\mu A\ cm^{-2}$ in the presence of 10 mM fructose) due to the presence of −OH groups on the electrode surface, which stabilize and orientate the enzyme layer on the electrode surface. The FDH/4-MPh/h-PG based electrode showed the best analytical performance with an excellent stability (90% retained activity over 90 days), a detection limit of 0.3 μM fructose, a linear range between 0.05 and 5 mM, and a sensitivity of 175 ± 15 $\mu A\ cm^{-2}\ mM^{-1}$. These properties were favorably compared with other fructose biosensors reported in the literature. The biosensor was successively tested to quantify the fructose content in food and beverage samples. No significant interference present in the sample matrixes was observed.

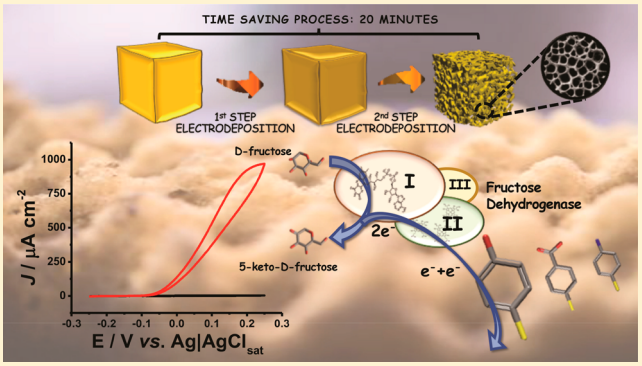

In the last few decades direct electron transfer (DET) reactions between redox enzymes and electrodes has been widely studied to gain insights into biological electron transfer mechanisms as well as to develop third generation biosensors and biofuel cells.[1−4] Although there are a lot of papers dealing with DET, most redox enzymes do not show DET properties mainly because the prosthetic (e.g., FAD, PQQ) and redox (e.g., heme *b*, heme *c*) cofactors are deeply buried within the protein structure.[2,5] Nevertheless, a lot of efforts have been addressed toward nanostructuration of electrode surfaces in order to improve DET reactions as an effect of enlarging the surface area, which would contribute to increasing the enzyme loading[6] as well as the possibility for chemical modification (e.g., self-assembled monolayer SAM, diazonium coupling, etc.) making a correct orientation of the enzyme possible onto the electrode surface minimizing the distance between the bound cofactor and the electrode surface.[7,8] A lot of nanomaterials have been exploited to improve DET[9,10] such as single- and multiwalled carbon nanotubes,[11] graphene,[12,13] highly-/nanoporous gold[14,15] and metal nanoparticles.[16−18] Among these nanomaterials, nanoporous gold (nPG, porous gold with pores in the nanometer range) electrodes represent a very promising alternative for the development of new implantable bioelectronics.[19] These electrodes exhibit remarkable properties such as high conductivity, large surface area, three-dimensional open porosity, and biocompatibility.[20] Besides the nPG electrodes, highly porous gold (h-PG) electrodes seem to be even more promising for the development of highly sensitive biosensors. h-PG electrodes present larger pores (micrometer range)

Received: July 10, 2018
Accepted: August 27, 2018
Published: August 27, 2018

DOI: 10.1021/acs.analchem.8b03093
Anal. Chem. 2018, 90, 12131−12136

Scheme 1. Schematic Representation of the Electrodeposition Method for h-PG Performed in Two Steps: Potential Sweeping for 25 Scans between +0.8 and 0 V vs Ag\|AgCl$_{sat}$ at a Scan Rate of 50 mV s^{-1}, Applying a Fixed Potential of −3 V vs Ag\|AgCl$_{sat}$ for 120 s in a 10 mM $AuCl_3$ Solution Containing 2.5 M NH_4Cl

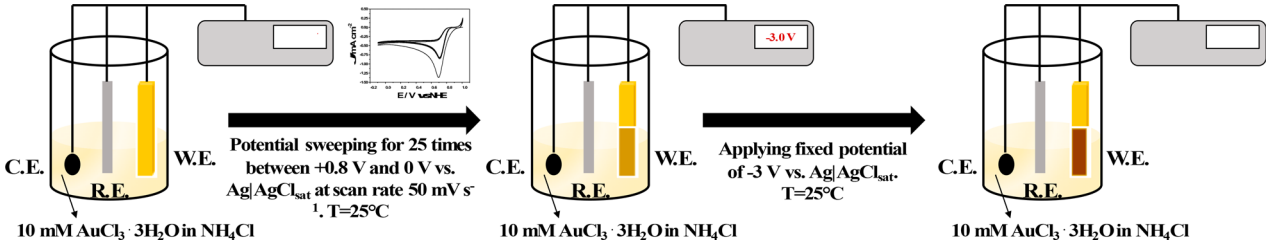

compared to nPG electrodes. In particular, each micropore presents an internal complex nanostructuration based on nanopores. As a consequence, h-PG electrodes show a very broad pore size distribution, drastically increasing the surface area and thus the current densities compared to the conventional nPG based electrodes.[21]

Generally, h-PG can be obtained by using mainly two approaches:[22] chemical dealloying or templating and self-templating methods. Chemical dealloying/etching is a corrosive process performed by dissolving metal elements such as Ag, Sn, and Cu in the alloy except for Au.[23,24] According to the chemical activity of the elements in the alloys, different reagents such as nitric acid, hydrochloric acid, or NaOH can be used.[25] Contrary to chemical dealloying, the templating method is a simple approach combining different techniques like flow-stream technique, sputter deposition, and electrochemical methods to create nanoporous gold films. In this method, there are three main steps: preparation of template, followed by deposition of gold, and then the removal of the template. Different templates can be used such as a layer of assembled particles, biologically made templates, or ion etched substrates. Polystyrene latex and silica particles have been widely used to make assembled particles as templates.[26−28] In contrast to previous methods, self-templating methods present two steps: gold electrodeposition and gas bubbling used as self-template. Accordingly we have developed a novel two step method, where first a layer of gold is electrodeposited onto the electrode surface followed by hydrogen bubbling at the electrode realized through applying a really negative potential in a solution containing NH_4Cl as supporting electrolyte and hydrogen source, as reported in Scheme 1. This technique is a really time saving and cost-effective way to produce highly porous gold avoiding all removal steps or chemical dissolution like in the dealloying procedures.[23,24,29,30]

Fructose dehydrogenase (FDH, EC 1.1.99.11) from *Gluconobacter japonicus* has been widely exploited to develop fructose biosensors based on both mediated and direct electron transfer[30−40] as well as bioanodes for enzymatic fuel cells (EFCs).[41−46] FDH is a membrane-bound flavocytochrome oxidoreductase that belongs to the hemoflavoproteins family.[47] FDH from *Gluconobacter japonicus* NCBR 3260 is a heterotrimeric membrane-bound enzyme complex with a molecular mass of 146.4 kDa, consisting of three subunits, i.e., subunit I (DH_{FDH}), which is the catalytic domain with a covalently bound flavin adenine dinucleotide (FAD) cofactor, where D-fructose is involved in a $2H^+/2e^-$ oxidation to produce 5-dehydro-D-fructose; subunit II (CYT_{FDH}), which acts as a built-in electron acceptor with three heme *c* moieties covalently bound to the enzyme scaffold and two of them (heme c_1 and heme c_2) are involved a one-by-one electron transfer pathway; and subunit III, which is not involved in the electron transfer but plays a key role for the enzyme complex stability.[48−51]

The aim of this paper was to improve the DET rate between FDH and the electrode through the use of a novel developed highly porous gold electrode, driving the enzyme orientation through the electrostatic interaction between the enzyme and the different SAMs used. The h-PG electrodes were produced through a two-step process involving the electrodeposition of a gold layer followed by hydrogen bubbling at the electrode surface as a self-template. Three different platforms have been compared in order to investigate the effect of the surface charge on the catalytic efficiency, which in turn is expected to mirror the enzyme orientation: viz., FDH/4-MBA/h-PG, FDH/4-MPh/h-PG, and FDH/4-APh/h-PG. FDH/4-MPh/h-PG showed the best performance due to the correct orientation of the enzyme for DET directly related to the best correct orientation of the enzyme onto the electrode surface as a result of the interactions between the enzyme, which is slightly positively charged at pH 6 used for immobilization (the p*I* of FDH was calculated to be 6.59 from the structure of the enzyme), and the uncharged electrode surface due to the presence of the −OH groups of 4-MPh (pK_a (OH group) = 9.56 calculated according to the Hammett equation[52]) and to the role of the exposed −OH groups on the stabilization of the immobilized FDH layer on the electrode surface. The electrochemical characterization and optimization of the fructose biosensor obtained with the FDH/4-MPh/h-PG electrode are herein presented. Finally, the feasibility of the developed biosensor for *in situ* analysis was tested in real food samples.

EXPERIMENTAL SECTION

Reagents and Apparatus. 4-Mercaptobenzoic acid (4-MBA, pK_a 4.05 of −COOH group), 4-mercaptophenol (4-MPh, pK_a 9.81 of −OH group), 4-aminothiophenol (4-APh, pK_a 4.15 of $-NH_2$ group), ammonium chloride (NH_4Cl), sodium acetate (NaAc), hydrochloric acid (HCl), sodium hydroxide (NaOH), D-fructose, D-glucose, D-galactose, D-mannitol, ascorbic acid, gold chloride ($AuCl_3 \cdot H_2O$), 3-(*N*-morpholino)propanesulfonic acid (MOPS), sulfuric acid (H_2SO_4), and 2-amino-2-(hydroxymethyl)-1,3-propanediol (TRIS) were purchased from Sigma-Aldrich (St. Louis, MO). D-Fructose dehydrogenase from *Gluconobacter japonicus* (FDH; EC 1.1.99.11) was purified from the culture supernatant of *Gluconobacter japonicus* NBRC 3260 obtained from the National Institute of Technology and Evaluation (Nishinomiya, Hyogo Pref., Japan) and solubilized in PBS buffer pH 6 (50∼500 mM) containing 0.1 mM 2-mercaptoethanol and 0.1% v/v TritonX-100 (volumetric activity measured with potassium ferricyanide at pH 4.5 = 420 ± 30 U mL^{-1}, specific activity = 250 ± 30 U mg^{-1}, protein concentration = 1.7 ± 0.2 mg mL^{-1}). All solutions were prepared using Milli-Q

DOI: 10.1021/acs.analchem.8b03093
Anal. Chem. 2018, 90, 12131−12136

water (ρ = 18.2 MΩ cm at 25 °C; Total Organic Compounds (TOC) < 10 μg L^{-1}, Millipore, Molsheim, France). Electrochemical and SEM apparatus details are reported in the Supporting Information.

Electrode Modification. Polycrystalline gold electrodes (diameter = 1.6 mm, BASi, West Lafayette, IN) were modified by electrodeposition of highly porous gold (h-PG) by initially sweeping the potential for 25 scans between +0.8 and 0 V vs Ag|$AgCl_{sat}$ at a scan rate of 50 mV s^{-1} and then applying a fixed potential of −3 V vs Ag|$AgCl_{sat}$ in a 10 mM $AuCl_3$ solution containing 2.5 M NH_4Cl.

Then, the modified electrodes were activated in 0.5 M H_2SO_4 by running CVs between 0 and +1.7 vs Ag|$AgCl_{sat}$ at a scan rate of 0.1 V s^{-1} until a well-defined CV was obtained. The modified electrode was next incubated overnight in a 10 mM ethanol solution containing one of the thiols, 4-MBA, 4-MPh, or 4-APh, to form a SAM on the electrode surface. Then, the electrode was thoroughly rinsed with ethanol and dried under a N_2 stream. For the biomodification, 3 μL of an FDH solution (1.7 mg mL^{-1}) were drop-cast on the top of the thiol-modified h-PG electrode and allowed to react in a moisturized atmosphere for 2 h to avoid evaporation of the reactants. Finally, the electrode was gently rinsed with a 50 mM NaAc buffer (pH 4.5) in order to remove any possible unbound enzyme molecules.

Food Samples Collections and Pretreatment. Real samples (cola, honey, tomato juice, apple juice, pineapple juice, energy drink) were bought in a local supermarket and carefully diluted in 50 mM NaAc buffer at pH 4.5 in a ratio of 1:250, before the analysis, except for the honey samples, which required a particular pretreatment. Honey samples were transferred into a beaker and heated for 5 min at 60 °C, stirring occasionally with a spatula, and finally allowed to cool. Next the samples were carefully diluted in 50 mM NaAc buffer at pH 4.5 in a ratio of 1:250.[35,53] The results obtained for FDH/4-MPh/h-PG biosensor were compared with a commercially available enzymatic kit (K-FRUGL 02/17) purchased from Megazyme (Bray Business Park, Bray, Co. Wicklow, A98 YV29, Ireland).

RESULTS AND DISCUSSION

SEM and Electrochemical Characterization of Highly Porous Gold Electrodes (h-PG). SEM experiments have been carried out to investigate the morphology of the highly porous gold (h-PG) substrates. In Figure 1A–C it is possible to observe that the surfaces with deposited h-PG exhibit a multimodal distribution of well-defined pores, which have a diameter ranging from 5 to 25 μm. However, in order to prove unequivocally the improvements of our electrodeposition method, A_{real} was calculated by integrating the peak current related to the reduction of the gold oxide (∼+0.9 V vs Ag|$AgCl_{sat}$) obtained by running CVs in 0.5 M H_2SO_4 at a scan rate of 100 mV s^{-1}, as shown in Figure S-1 (Supporting Information). The theoretical charge density considered for reduction of gold oxide is 390 ± 10 μC cm^{-2}. Therefore, the Areal for the h-PG modified gold electrodes was 23.6 ± 0.8 cm^2, which is roughly 300 times higher compared to the bare gold electrodes (0.08 ± 0.01 cm^2).

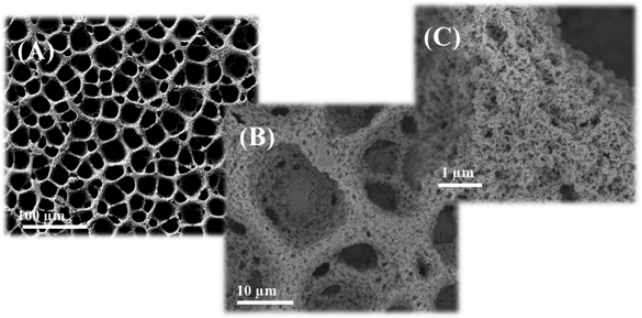

Figure 1. SEM images at different magnifications (A) 100 μm, (B) 10 μm, and (C) 1 μm of the h-PGE obtained through a two step electrodeposition protocol: (i) sweeping the potential for 25 scans between +0.8 and 0 V vs Ag|$AgCl_{sat}$, (ii) applying a fixed potential of −3 V vs Ag|$AgCl_{sat}$ for 120 s; both steps have been carried out in 10 mM $AuCl_3 \cdot H_2O$ containing 2.5 M NH_4Cl.

Electrochemical Characterization of FDH Immobilized on Self-Assembled Monolayer (SAM) Modified h-PG Electrodes. After preliminary characterization, the h-PG electrodes were further modified with one of three different thiols, *viz.*, 4-MBA, 4-MPh, and 4-APh, to form self-assembled monolayers (SAMs) on the surface in order to investigate the effect of electrostatic attraction/repulsion between the differently charged electrode surfaces and FDH expected to control the enzyme orientation.[54,55] In a series of previously published papers, it has been proven that the orientation of a redox enzyme is a key issue to obtain efficient direct electron transfer (DET) communication between the enzyme active site and the electrode due to the enzyme structure, the position of both the prosthetic and other redox groups, and the enzyme surface charge (isoelectric point).[2,56−58]

Figure S-2A shows the CV for the FDH/4-MBA/h-PG modified electrode under nonturnover conditions (50 mM NaAc buffer pH 4.5), where it is possible to observe a tendency for a couple of waves with a midpoint potential ($E^{\circ\prime}$) of +0.045 vs Ag|$AgCl_{sat}$, which is actually close to the value reported in the literature for heme c_2 (+0.060 V vs Ag|$AgCl_{sat}$).[59] In the presence of 10 mM D-fructose as substrate the FDH/4-MBA/h-PG electrode showed a slight electrocatalytical wave starting at E_{ONSET}= −0.070 V vs Ag|$AgCl_{sat}$ rising up to 100 μA cm^{-2} at 0.2 V vs Ag|$AgCl_{sat}$, as seen in Figure 2A.

In contrast, the CV of the FDH/4-MPh/h-PG modified electrode showed two clear couples of redox waves in 50 mM NaAc buffer pH 4.5, as depicted in Figure S-2B. The more negative redox couple showed an $E^{\circ\prime}$ value of −0.032 vs Ag|$AgCl_{sat}$, while the other one of +0.068 vs Ag|$AgCl_{sat}$, which are in good agreement with the values reported in the literature for heme c_1 (−0.010 V vs Ag|$AgCl_{sat}$) and heme c_2 (+0.060 V vs Ag|$AgCl_{sat}$), respectively.[59] Furthermore, with the addition of substrate (10 mM D-fructose), the electrode exhibits a great electrocatalytical wave starting at E_{ONSET} = −0.115 V vs Ag|$AgCl_{sat}$ rising up to 920 μA cm^{-2} at 0.2 V vs Ag|$AgCl_{sat}$, as reported in Figure 2B.

In the last case, the FDH/4-APh/h-PG electrode was scanned under nonturnover conditions (50 mM NaAc buffer pH 4.5), showing a nonreversible electrochemistry of FDH with only two oxidation peaks at +0.032 V vs Ag|$AgCl_{sat}$ and +0.122 V vs Ag|$AgCl_{sat}$, which might correspond to heme c_2 and heme c_3, as reported in Figure S-2C. Most probably the electrochemistry of the enzyme showed an irreversible process probably due to the unfavorable orientation obtained on the slight positive charged/uncharged surface. Nevertheless, the CV in the presence of substrate showed an electrocatalytical wave starting at E_{ONSET} = −0.098 V vs Ag|$AgCl_{sat}$ rising up to 314 μA cm^{-2} at 0.2 V vs Ag|$AgCl_{sat}$, as shown in Figure 2C.

Moreover for comparison, also the FDH/h-PG electrode was scanned with CV under nonturnover conditions (50 mM NaAc

DOI: 10.1021/acs.analchem.8b03093
Anal. Chem. 2018, 90, 12131−12136

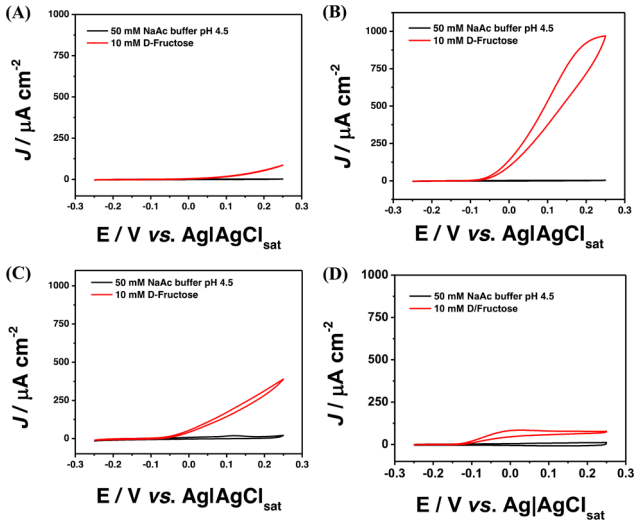

Figure 2. (A) CVs of FDH/4-MBA/h-PG in absence (black curve) and in the presence of 10 mM D-fructose (red curve); (B) CVs of FDH/4-MPh/h-PG in absence (black curve) and in the presence of 10 mM D-fructose (red curve); (C) CVs of FDH/4-APh/h-PG in absence (black curve) and in the presence of 10 mM D-fructose (red curve); (D) CVs of FDH/h-PG in absence (black curve) and in the presence of 10 mM D-fructose (red curve). Experimental conditions: 50 mM NaAc buffer at pH 4.5, scan rate 5 mV s^{-1}, T = 25 °C.

buffer pH 4.5), exhibiting two oxidation peaks at +0.072 V vs Ag|$AgCl_{sat}$ and +0.176 V vs Ag|$AgCl_{sat}$, which might correspond to heme c_2 and heme c_3, as reported in Figure S-2D. Most probably the electrochemistry of the enzyme showed an irreversible process probably due to its random orientation. Nevertheless, the CV in the presence of substrate showed an electrocatalytical wave starting at E_{ONSET} = −0.131 V vs Ag|$AgCl_{sat}$ rising up to 79 μA cm^{-2} at 0.2 V vs Ag|$AgCl_{sat}$, as shown in Figure 2D.

According to these results, it was possible to establish FDH/4-MPh/h-PG as the best modified electrodes due to the quasi-reversible behavior, clearly visible in nonturnover electrochemistry, the great electrocatalytical behavior, and the amount of FDH immobilized. These results are related to the best correct orientation of the enzyme onto the electrode surface as a result of the interactions between the enzyme, which is slightly positively charged at pH 6 used for immobilization (the pI of FDH was calculated to be 6.59 from the structure of the enzyme), and the uncharged electrode surface due to the presence of −OH groups of 4-MPh (pK_a (OH group) = 9.56 calculated according to the Hammett equation), which are well-known to stabilize the enzyme layer.

Fructose Biosensor Development. To investigate the electroanalytical and kinetic parameters of FDH/4-MBA/h-PG, FDH/4-MPh/h-PG, and FDH/4-APh/h-PG, the amperometric responses toward D-fructose have been recorded by using the flow injection system (FIA) approach injecting D-fructose solutions at different concentrations, shown in Figure 3A. As expected from the results exhibited in Figure 3A, the FDH/4-MPh/h-PG modified electrode showed a faster and a much higher peak response (3 s) compared to FDH/4-MBA/h-PG and FDH/4-APh/h-PG, which exhibit a response time of 8 s and a much lower current response. The calibration curves exhibited a linear response range between 0.05 and 5 mM (R^2 = 0.99, n = 5) and with the following sensitivities: 175 ± 15 μA mM^{-1} cm^{-2} for FDH/4-MPh/h-PG, 60 ± 3 μA mM^{-1} cm^{-2} for FDH/4-APh/h-PG, and 14 ± 1 μA mM^{-1} cm^{-2} for FDH/4-MBA/h-PG, respectively, as shown in the inset of Figure 3A. At higher concentrations than 5 mM the amperometric response is no longer linear due to the saturation of the enzyme active site. The detection limit resulted in 0.3 μM for FDH/4-MPh/h-PG, 1.2 μM for FDH/4-APh/h-PG, and 1.5 μM for FDH/4-MBA/h-PG, respectively, calculated using the relation 3σ/S, where σ is the absolute standard deviation of the intercept and S is the slope of the calibration curve.[60] The electroanalytical and kinetic

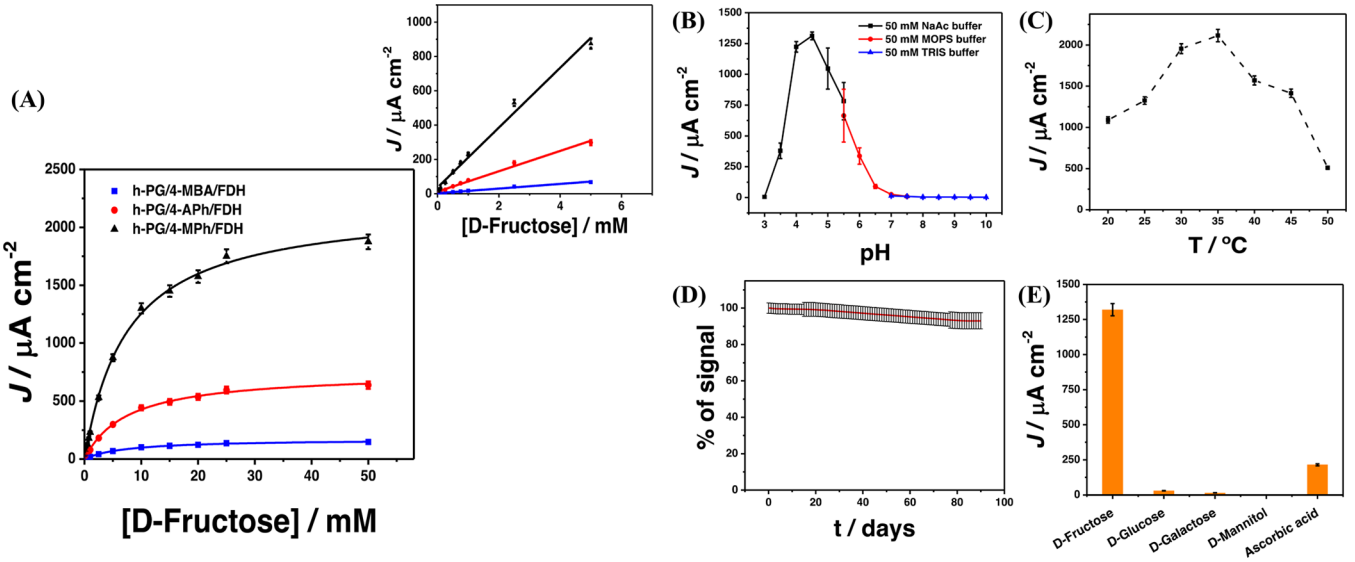

Figure 3. (A) D-Fructose biosensor calibration graph of FDH/4-APh/hPG (red), FDH/4-MPh/h-PG (black), FDH/4-MBA/h-PG (blue) in 50 NaAc buffer pH 4.5. Insert: linear range; (B) FDH/4-MPh/h-PG biosensor response over the pH range (4.5−10): 50 mM acetate buffer (black), 50 mM MOPS buffer (red), and in 50 mM TRIS buffer (blue), with E_{app} = 0.250 vs Ag|$AgCl_{sat}$; flow rate 0.5 mL min^{-1}; (C) FDH/4-MPh/h-PG biosensor response over the T range (20−45 °C) in TRIS buffer; (D) lifetime FDH/4-MPh/h-PG biosensor in the presence of 10 mM D-fructose solution; (E) influence of interfering compounds on fructose response in the presence of 10 mM D-glucose, D-galactose, D-mannitol, and ascorbic acid. Experimental conditions: 50 mM NaAc buffer E_{app} = 0.250 vs Ag|$AgCl_{sat}$; flow rate 0.5 mL min^{-1}; injection volume 50 μL; T = 25 °C.

DOI: 10.1021/acs.analchem.8b03093
Anal. Chem. 2018, 90, 12131−12136

parameters for FDH/4-MBA/h-PG, FDH/4-MPh/h-PG, and FDH/4-APh/h-PG electrodes are reported in Table S-1. The apparent kinetic parameters (I_{max}, K_M^{app}) are in good agreement with the values reported in the literature for nanostructured biosensors for fructose detection based on DET.[49,59] The analytical results of the FDH/4-MPh/h-PG electrode were further compared with other platforms reported in the literature showing great improvements when comparing sensitivity, linear range, detection limit, selectivity, and stability (Table S-2).[30,31,35,61−63]

Effect of pH, Temperature, Interferences, and Stability Studies. Since the FDH/4-MPh/h-PG electrode platform exhibits the best analytical performance compared to the others, the effects of pH and temperature have been evaluated only for this platform. The effects of pH and temperature are shown in Figure 3B,C. The optimum pH was found to be pH 4.5 in 50 mM NaAc buffer at a temperature of 35 °C. The catalytic current density rapidly decreased when increasing the pH revealing only one optimum pH at 4.5 in the investigated pH range of 3 and 10, in perfect agreement with the results reported in the literature.[63] Concerning the temperature dependence, the FDH/4-MPh/h-PG electrode showed its best performance at 35 °C.

Nevertheless, the biosensor still exhibits good performance both at room temperature and at 45 °C, while at 50 °C the current density was drastically decreased probably due to denaturation of the enzyme. The modified biosensor seems to retain more than 90% of its initial activity after 90 days, probably due to the high stability of the enzyme layer directly related to the nanostructuration of the electrode surface with the electrodeposition of h-PG, as shown in Figure 3D. Nevertheless, we should consider that the −OH groups exposed on the electrode surface create a favorable environment for the immobilization of a membrane bound protein namely FDH.

Finally, the selectivity of the proposed biosensor was studied in order to see the influence of possible interfering compounds generally present in food samples such as D-glucose, D-galactose, D-mannitol, and ascorbic acid. The signal obtained for a fixed concentration of D-fructose (10 mM) was compared to that obtained with a sample containing the same D-fructose concentration plus equal concentrations of the potential interfering compounds. The amperometric signal is lower than 10% for all the compounds tested except for ascorbic acid (about 20%), as reported in Figure 3E, which may interfere in real measurements because of its direct oxidation on the electrode surface occurring approximately at 0.2 V vs AglAgCl$_{sat}$ close to formal potential of L-ascorbic acid oxidation ($E^{\circ\prime}$ = +0.170 V vs AglAgCl$_{sat}$).[64]

Fructose Detection in Food Samples. To demonstrate the feasibility of the modified electrode for the *in situ* detection of D-fructose as a screening method for analytical process control in food samples, the proposed biosensor was used to detect the concentration of D-fructose in samples collected and used according to the procedure reported in section Food Samples Collections and Pretreatment, (referred to protocols reported in the literature and provided with guidelines of the spectrophotometric reference method). The reliability of the FDH/4-MPh/h-PG electrode platform was evaluated by comparing the results with those obtained with the spectrophotometric reference method. The proposed biosensor exhibits satisfactory results in all food samples with a recovery percentage above 94% (RSD values lower than 2.5%, see Table S-3).

CONCLUSIONS

This paper demonstrated the possibility to achieve efficient DET for FDH immobilized within the FDH/4-MPh/h-PG platform as a result of the highly porous gold electrode in combination with the exposed −OH groups of the SAM. The latter is responsible for the correct orientation of FDH onto the electrode surface due the stabilization effect of the exposed −OH groups of the SAM on membrane bound protein like FDH. The proposed biosensor based on the FDH/4-MPh/h-PG platform showed a really high catalytic current density of 920 μA cm^{-2} at 0.2 V vs AglAgCl$_{sat}$, with a great improvement compared with the other platforms reported in the literature. The FDH/4-MPh/h-PG biosensor can be easily prepared through a two-step electrodeposition protocol (20 min), further modified with 4-mercaptophenol to form a SAM, and finally with the enzyme deposition. The fructose biosensor was fast-responding, showed a great stability (more than 90% of retained signal after 90 days), selectivity, and sensitivity (175 ± 15 μA mM^{-1} cm^{-2}) with the lowest detection limit (0.3 μM). According to these results, the proposed electrode platform, namely, FDH/4-MPh/h-PG exhibits great promises both as a third generation biosensor for fructose detection and as a biofuel cell anode suitable to be integrated in industrial processes.

ASSOCIATED CONTENT

Supporting Information

The Supporting Information is available free of charge on the ACS Publications website at DOI: 10.1021/acs.analchem.8b03093.

Experimental apparatus, cleaning and activation procedures for gold electrodes, CVs, electroanalytical and kinetic parameters, comparison with fructose biosensors reported in the literature, and results relative to the analysis of real food and beverage samples obtained with FDH/4-MPh/h-PG biosensor and a commercially available enzymatic kit (PDF)

AUTHOR INFORMATION

Corresponding Author

*E-mail: paolo.bollella@uniroma1.it.

ORCID

Paolo Bollella: 0000-0001-9049-6406

Kenji Kano: 0000-0002-4667-7020

Lo Gorton: 0000-0002-7278-0478

Author Contributions

Dr. Paolo Bollella performed the experimental measurements and wrote the manuscript. Dr. Yuya Hibino and Prof. Kenji Kano kindly provided the enzyme fructose dehydrogenase from *Gluconobacter japonicus*. Prof. Lo Gorton and Prof. Riccarda Antiochia carefully revised the manuscript. All authors have given approval to the final version of the manuscript.

Notes

The authors declare no competing financial interest.

ACKNOWLEDGMENTS

Dr. Crispin Hetherington (Lund University, Department of Chemistry, The National Center for High-Resolution Electron Microscopy nCHREM) is particular acknowledged for help with SEM investigation of the highly porous gold electrodes. The authors would like to thank for the following agencies for financial funding: The Swedish Research Council (Vetenskaps-

DOI: 10.1021/acs.analchem.8b03093
Anal. Chem. 2018, 90, 12131−12136

rådet Project 2014-5908), the European Commission (Project "Bioenergy" FP7-PEOPLE-2013-ITN-607793), and a scholarship of the Erasmus+ Project Unipharma-Graduates, promoted by a Consortium of Italian Universities and coordinated by Sapienza University of Rome.

REFERENCES

(1) Falk, M.; Blum, Z.; Shleev, S. *Electrochim. Acta* **2012**, *82*, 191−202.
(2) Gorton, L.; Lindgren, A.; Larsson, T.; Munteanu, F.; Ruzgas, T.; Gazaryan, I. *Anal. Chim. Acta* **1999**, *400*, 91−108.
(3) Ferapontova, E. E.; Shleev, S.; Ruzgas, T.; Stoica, L.; Christenson, A.; Tkac, J.; Yaropolov, A. I.; Gorton, L. In *Electrochemistry of Nucleic Acids and Proteins: Towards Electrochemical Sensors for Genomics and Proteomics*; Palecek, E., Scheller, F., Wang, J., Eds.; Elsevier: Amsterdam, The Netherlands, 2005; pp 517−598.
(4) Bollella, P.; Gorton, L.; Antiochia, R. *Sensors* **2018**, *18*, 1319.
(5) Frew, J. E.; Hill, H. A. O. *Eur. J. Biochem.* **1988**, *172*, 261−269.
(6) Holzinger, M.; Le Goff, A.; Cosnier, S. *Front. Chem.* **2014**, *2*, 63−63.
(7) Gooding, J. J.; Ciampi, S. *Chem. Soc. Rev.* **2011**, *40*, 2704−2718.
(8) Chekin, F.; Gorton, L.; Tapsobea, I. *Anal. Bioanal. Chem.* **2015**, *407*, 439−446.
(9) Mazzei, F.; Favero, G.; Bollella, P.; Tortolini, C.; Mannina, L.; Conti, M. E.; Antiochia, R. *Int. J. Environ. Health* **2015**, *7*, 267−291.
(10) Bollella, P.; Ludwig, R.; Gorton, L. *Appl. Mater. Today* **2017**, *9*, 319−332.
(11) Gooding, J. J. *Electrochim. Acta* **2005**, *50*, 3049−3060.
(12) Bollella, P.; Fusco, G.; Tortolini, C.; Sanzò, G.; Favero, G.; Gorton, L.; Antiochia, R. *Biosens. Bioelectron.* **2017**, *89*, 152−166.
(13) Carbone, M.; Gorton, L.; Antiochia, R. *Electroanalysis* **2015**, *27*, 16−31.
(14) Sanzó, G.; Taurino, I.; Antiochia, R.; Gorton, L.; Favero, G.; Mazzei, F.; De Micheli, G.; Carrara, S. *Bioelectrochemistry* **2016**, *112*, 125−131.
(15) Du Toit, H.; Di Lorenzo, M. *Sens. Actuators, B* **2014**, *192*, 725−729.
(16) Bollella, P.; Schulz, C.; Favero, G.; Mazzei, F.; Ludwig, R.; Gorton, L.; Antiochia, R. *Electroanalysis* **2017**, *29*, 77−86.
(17) Bollella, P.; Gorton, L.; Ludwig, R.; Antiochia, R. *Sensors* **2017**, *17*, 1912.
(18) Kizling, M.; Dzwonek, M.; Wieckowska, A.; Bilewicz, R. *Curr. Opin. Electrochem.* **2018**, DOI: 10.1016/j.coelec.2018.05.021.
(19) Bollella, P.; Gorton, L. *Curr. Opin. Electrochem.* **2018**, *10*, 157.
(20) Dixon, M. C.; Daniel, T. A.; Hieda, M.; Smilgies, D. M.; Chan, M. H.; Allara, D. L. *Langmuir* **2007**, *23*, 2414−2422.
(21) Li, Y.; Song, Y.-Y.; Yang, C.; Xia, X.-H. *Electrochem. Commun.* **2007**, *9*, 981−988.
(22) Zhang, R.; Olin, H. *Materials* **2014**, *7*, 3834−3854.
(23) Siepenkoetter, T.; Salaj-Kosla, U.; Xiao, X.; Belochapkine, S.; Magner, E. *Electroanalysis* **2016**, *28*, 2415−2423.
(24) Xiao, X.; Si, P.; Magner, E. *Bioelectrochemistry* **2016**, *109*, 117−126.
(25) Ding, Y.; Kim, Y. J.; Erlebacher, J. *Adv. Mater.* **2004**, *16*, 1897−1900.
(26) Gloria, D.; Gooding, J. J.; Moran, G.; Hibbert, D. B. *J. Electroanal. Chem.* **2011**, *656*, 114−119.
(27) Ben-Ali, S.; Cook, D. A.; Evans, S. A. G.; Thienpont, A.; Bartlett, P. N.; Kuhn, A. *Electrochem. Commun.* **2003**, *5*, 747−751.
(28) Szamocki, R.; Reculusa, S.; Ravaine, S.; Bartlett, P. N.; Kuhn, A.; Hempelmann, R. *Angew. Chem., Int. Ed.* **2006**, *45*, 1317−1321.
(29) Plowman, B. J.; Jones, L. A.; Bhargava, S. K. *Chem. Commun.* **2015**, *51*, 4331−4346.
(30) Siepenkoetter, T.; Salaj-Kosla, U.; Magner, E. *ChemElectroChem* **2017**, *4*, 905−912.
(31) Antiochia, R.; Gorton, L. *Sens. Actuators, B* **2014**, *195*, 287−293.
(32) Antiochia, R.; Vinci, G.; Gorton, L. *Food Chem.* **2013**, *140*, 742−747.
(33) Antiochia, R.; Lavagnini, I.; Magno, F. *Anal. Lett.* **2004**, *37*, 1657−1669.
(34) Kizling, M.; Draminska, S.; Stolarczyk, K.; Tammela, P.; Wang, Z.; Nyholm, L.; Bilewicz, R. *Bioelectrochemistry* **2015**, *106*, 34−40.
(35) Parellada, J.; Domínguez, E.; Fernández, V. M. *Anal. Chim. Acta* **1996**, *330*, 71−77.
(36) Begum, A.; Kobatake, E.; Suzawa, T.; Ikariyama, Y.; Aizawa, M. *Anal. Chim. Acta* **1993**, *280*, 31−36.
(37) Khan, G. F.; Shinohara, H.; Ikariyama, Y.; Aizawa, M. *J. Electroanal. Chem. Interfacial Electrochem.* **1991**, *315*, 263−273.
(38) Khan, G. F.; Shinohara, H.; Ikariyama, Y.; Aizawa, M. *Sens. Actuators, B* **1993**, *14*, 673−674.
(39) Tominaga, M.; Nomura, S.; Taniguchi, I. *Biosens. Bioelectron.* **2009**, *24*, 1184−1188.
(40) Tominaga, M.; Shirakihara, C.; Taniguchi, I. *J. Electroanal. Chem.* **2007**, *610*, 1−8.
(41) Ikeda, T.; Kano, K. *J. Biosci. Bioeng.* **2001**, *92*, 9−18.
(42) Kamitaka, Y.; Tsujimura, S.; Setoyama, N.; Kajino, T.; Kano, K. *Phys. Chem. Chem. Phys.* **2007**, *9*, 1793−1801.
(43) Sakai, H.; Nakagawa, T.; Tokita, Y.; Hatazawa, T.; Ikeda, T.; Tsujimura, S.; Kano, K. *Energy Environ. Sci.* **2009**, *2*, 133−138.
(44) Meredith, M. T.; Minson, M.; Hickey, D.; Artyushkova, K.; Glatzhofer, D. T.; Minteer, S. D. *ACS Catal.* **2011**, *1*, 1683−1690.
(45) Miyake, T.; Yoshino, S.; Yamada, T.; Hata, K.; Nishizawa, M. *J. Am. Chem. Soc.* **2011**, *133*, 5129−5134.
(46) Murata, K.; Kajiya, K.; Nakamura, N.; Ohno, H. *Energy Environ. Sci.* **2009**, *2*, 1280−1285.
(47) Bollella, P.; Hibino, Y.; Kano, K.; Gorton, L.; Antiochia, R. *Anal. Bioanal. Chem.* **2018**, *410*, 3253−3264.
(48) Kawai, S.; Goda-Tsutsumi, M.; Yakushi, T.; Kano, K.; Matsushita, K. *Appl. Environ. Microbiol.* **2013**, *79*, 1654−1660.
(49) Tsujimura, S.; Nishina, A.; Hamano, Y.; Kano, K.; Shiraishi, S. *Electrochem. Commun.* **2010**, *12*, 446−449.
(50) Hibino, Y.; Kawai, S.; Kitazumi, Y.; Shirai, O.; Kano, K. *Electrochem. Commun.* **2017**, *77*, 112−115.
(51) Kawai, S.; Kitazumi, Y.; Shirai, O.; Kano, K. *Electrochim. Acta* **2016**, *210*, 689−694.
(52) Lide, D. R. *CRC Handbook of Chemistry and Physics*, 90th ed.; Taylor & Francis, 2009.
(53) Piermarini, S.; Volpe, G.; Esti, M.; Simonetti, M.; Palleschi, G. *Food Chem.* **2011**, *127*, 749−754.
(54) Ferretti, S.; Paynter, S.; Russell, D. A.; Sapsford, K. E.; Richardson, D. J. *TrAC, Trends Anal. Chem.* **2000**, *19*, 530−540.
(55) Gooding, J. J.; Hibbert, D. B. *TrAC, Trends Anal. Chem.* **1999**, *18*, 525−533.
(56) Matsumura, H.; Ortiz, R.; Ludwig, R.; Igarashi, K.; Samejima, M.; Gorton, L. *Langmuir* **2012**, *28*, 10925−10933.
(57) Blanford, C. F.; Heath, R. S.; Armstrong, F. A. *Chem. Commun.* **2007**, 1710−1712.
(58) Tasca, F.; Harreither, W.; Ludwig, R.; Gooding, J. J.; Gorton, L. *Anal. Chem.* **2011**, *83*, 3042−3049.
(59) Kawai, S.; Yakushi, T.; Matsushita, K.; Kitazumi, Y.; Shirai, O.; Kano, K. *Electrochem. Commun.* **2014**, *38*, 28−31.
(60) Shrivastava, A.; Gupta, V. *Chron. Young Sci.* **2011**, *2*, 21−21.
(61) Campuzano, S.; Galvez, R.; Pedrero, M.; de Villena, F. J. M.; Pingarrón, J. M. *Anal. Bioanal. Chem.* **2003**, *377*, 600−607.
(62) Kinnear, K. T.; Monbouquette, H. G. *Anal. Chem.* **1997**, *69*, 1771−1775.
(63) Damar, K.; Demirkol, D. O. *Talanta* **2011**, *87*, 67−73.
(64) Rueda, M.; Aldaz, A.; Sanchez-Burgos, F. *Electrochim. Acta* **1978**, *23*, 419−424.

DOI: 10.1021/acs.analchem.8b03093
Anal. Chem. 2018, 90, 12131−12136